Stereoretentive Chlorination of Cyclic Alcohols Catalyzed by Titanium(IV) Tetrachloride: Evidence for a Front Side Attack Mechanism

Deboprosad Mondal,[†] Song Ye Li,[†] Luca Bellucci,*,[‡] Teodoro Laino,[§] Andrea Tafi,[∥] Salvatore Guccione,[⊥] and Salvatore D. Lepore*,[†]

[†]Department of Chemistry, Florida Atlantic University, Boca Raton, Florida 33431, United States
[‡]Center S3, CNR Institute of Nanoscience, Via Campi 213/A, I-41125 Modena, Italy
[§]IBM Zurich Research Laboratory, CH-8803 Rüeschlikon, Switzerland
[∥]Dipartimento Farmaco Chimico Tecnologico, Università degli Studi di Siena, I-53100 Siena, Italy
[⊥]Dipartimento di Scienze del Farmaco, Università degli Studi di Catania, I-95125 Catania, Italy

Ⓢ *Supporting Information*

ABSTRACT: A mild chlorination reaction of alcohols was developed using the classical thionyl chloride reagent but with added catalytic titanium(IV) chloride. These reactions proceeded rapidly to afford chlorination products in excellent yields and with preference for retention of configuration. Stereoselectivities were high for a variety of chiral cyclic secondary substrates including sterically hindered systems. Chlorosulfites were first generated in situ and converted to alkyl chlorides by the action of titanium tetrachloride which is thought to chelate the chlorosulfite leaving group and deliver the halogen nucleophile from the front face. To better understand this novel reaction pathway, an ab initio study was undertaken at the DFT level of theory using two different computational approaches. This computational evidence suggests that while the reaction proceeds through a carbocation intermediate, this charged species likely retains pyramidal geometry existing as a conformational isomer stabilized through hyperconjugation (hyperconjomers). These carbocations are then essentially "frozen" in their original configurations at the time of nucleophilic capture.
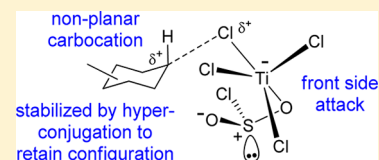
INTRODUCTION

Though often a final product in itself, alcohols are among the most common and important synthesis intermediates in organic and medicinal chemistry lending importance to the search for mild and high-yielding functional group interconversions for this compound class.[1] In this regard, the chloro-dehydroxylation of aliphatic alcohols has long been recognized as a valuable transformation prompting the development of a plethora of techniques[2] including the classical thionyl chloride reaction.[3] The challenging aspect in the development of these reactions with chiral alcohols often centers on issues of stereospecificity attracting the attention of numerous researchers in the past decade.[4]

Thionyl chloride is widely used in organic synthesis especially for the conversion of alcohols to their corresponding chlorides often under reflux conditions. This reagent is often preferable to other reagents due to its gaseous byproduct (SO_2) for simplified purification. Excess thionyl chloride also can be readily removed by distillation or evaporation. However, this reaction often requires less than mild conditions, thus limiting its application in the synthesis of delicate molecules. Traditional alcohol chlorination reactions with thionyl chloride are thought to involve either inversion or retention of configuration depending on the involvement of the reaction solvent.[5] In these systems, retention of configuration is achieved mecha-

nistically through a double inversion in the presence of nucleophilic solvents. For secondary chiral alcohols, whether this reaction proceeds via an internal nucleophilic substitution ($S_N i$) with stereoretention through ionic or concerted mechanism is still under debate.[6]

For several years, we have been interested in the development of highly efficient leaving groups containing chelating units capable of attracting incoming nucleophiles. In our previous study, we demonstrated that the halogenations of cyclic secondary alcohols containing nucleophile assisting leaving groups (NALGs) react at greatly accelerated rates with predominant retention of configuration.[7] Following a similar line of thinking, we have recently developed a new one-pot mild amidation method using an in situ formed chlorosulfite, derived from thionyl chloride.[8] As part of that amidation work we observed a tendency of titanium(IV) species to catalyze the conversion of chlorosulfites to chlorides at low temperatures. Herein we describe these findings and further explore the preference in this chlorination reaction for retention of configuration with cyclic alcohols.[8] To shed light on the reaction mechanism, we also include our computational

investigation aimed at weighing the most probable paths of the reaction through the characterization of their transition states (TS) using density functional theory (DFT).

■ RESULTS AND DISCUSSION

Chlorination Studies. Owing to its propensity to form hydride shift and elimination products, we began our chlorination studies with *l*-menthol. This alcohol was first treated with thionyl chloride at 0 °C to form the chlorosulfite, which remained stable at this temperature as well as at room temperature even after 24 h. The subsequent addition of catalytic amounts of TiCl$_4$ led to the chlorinated product with retention of configuration with no tertiary chloride product observed (Scheme 1). In general, these reactions gave product

Scheme 1. Chlorination of *l*-Menthol with SOCl$_2$ and Catalytic TiCl$_4$
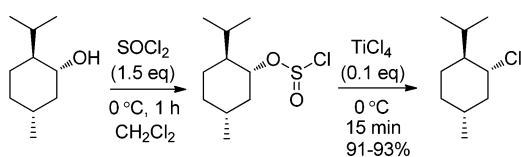
in high yields within 15 min at 0 °C with as little as 10 mol % of TiCl$_4$. When the reaction was cooled to −78 °C, after chlorosulfite formation, the chlorination reaction time increased to over 2 h even with 200 mol % of the titanium reagent. Preliminary data also reveal that the present titanium(IV) methodology can be extended to bromination. For example, the bromide of *l*-menthol was obtained in 81% yield with complete retention of configuration using SOBr$_2$ and TiBr$_4$ (10%) at 0 °C in dichloromethane.[9]

The use of catalytic TiCl$_4$ with chlorosulfites was then explored for a variety of cyclic secondary alcohols. Yields and stereoselectivities were high in all cases, including traditionally problematic sterically hindered systems (Table 1). As with menthol, nearly complete retention of configuration was also observed for many chiral cyclic alcohols (entries 6−10).[10] Under these catalytic conditions, the chlorosulfites of tertiary alcohols led to mixtures of elimination and chlorination products with the exception of 1-admantanol, which afforded only chloride product in 88% yield (entry 5). It should be noted that 2-methylcyclohexanol (as well as *l*-menthol) gave no tertiary chloride product, which would have been expected if a classical carbocation mechanism were operative (entry 6).[11]

We initially found *cis*-3,3,5-trimethylcyclohexanol and β-cholestanol to give some inversion product using our catalytic conditions. Under these conditions (10% TiCl$_4$), the trimethylcyclohexanol and cholestanol derivatives gave 12% and 29% inversion products, respectively. However, when the reaction concentration was diluted (from 1.0 to 0.1 M) and excess equivalents of TiCl$_4$ were employed, the chlorination reaction gave only products with retention of configuration (Table 2).

Our chlorination studies of the *cis/trans* isomers of 3-methylcyclohexanol and 4-methylcyclohexanol (Tables 3 and 4) led to mixtures of products. Specifically, we observed a small amount of inversion products along with varying amounts of hydride shift products. As with other substrates, an excess of TiCl$_4$ (2 equiv) seemed critical for optimal results. Additional studies revealed that improved yields of stereoretentive products can be achieved at colder temperatures (−78 °C)

Table 1. Generality Study of One-Pot Chlorination of Various Alcohols: All Chiral Alcohols Lead to Chlorination Products with Exclusive Retention of Configuration


^{a}Isolated yields. ^{b}Yield based on NMR. ^{c}For exclusive stereoretention, 2.0 equiv of TiCl$_4$ was required. ^{d}For exclusive stereoretention, 5.0 equiv of TiCl$_4$ was required.

Table 2. Chlorination of *cis*-3,3,5-Trimethylcyclohexanol (7) and β-Cholestanol (9)

entry	ROH	conc (M)	temp (°C)	time (h)	TiCl$_4$ (equiv)	ret/inv^a	yield^b (%)
1	7	1.0	0	5.0	0.10	7.1:1.0	75
2	7	1.0	0	1.0	2.0	ret only	80
3	7	0.1	0	3.0	2.0	ret only	80
4	7	0.1	−78	15	2.0	ret only	75
5	9	1.0	0	0.25	0.10	2.5:1.0	88
6	9	0.1	0	0.25	0.10	2.5:1.0	90
7	9	0.1	−78	10	2.0	2.5:1.0	92
8	9	0.1	0	0.25	5.0	ret only	80
9	9	0.1	0	0.25	10	ret only	72

^{a}Retention/inversion ratios determined by NMR. ^{b}Isolated yields.

and a reaction concentration of the alcohol substrates maintained at 0.1 M. For example, *cis*-3-methyl cyclohexanol (**12**) led to a 7:1 ratio (retention: inversion) of chlorination products with catalytic TiCl$_4$ (10%) at 0 °C (Table 3).

Table 3. Chlorination Results with *trans*-3-Methylcyclohexanol (11) and *cis*-3-Methylcyclohexanol (12)
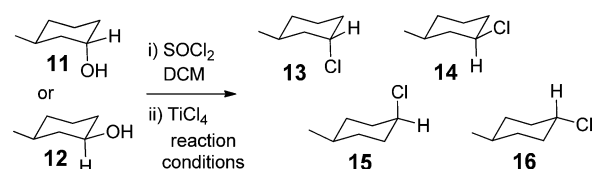
entry	ROH	conc (M)	temp (°C)	time (h)	TiCl$_4$ (equiv)	13:14:15:16[a]	yield[b] (%)
1	12	1.0	0	0.50	0.10	5.0:36:1.0:0	75
2	12	1.0	−78	8.0	2.0	1.1:11:1.0:0	73
3	12	0.1	0	0.50	2.0	4.4:52:1.0:0	78
4	12	0.1	−78	12	2.0	ret only	70
5	11	0.1	0	0.50	2.0	4.7:1.1:4.8:1.0	62
6	11	0.1	−78	12	2.0	1.1:1:1.0:0	65

[a]Ratios determined by NMR. [b]Isolated yields. Relatively low yields likely due to product volatility since NMR analysis of crude indicates near-quantitative conversion to the corresponding chloride.

However, exclusive retention of configuration in the product was obtained with 2 equivalents of the Lewis acid at −78 °C. These optimized conditions also suppressed inversion product with *trans*-isomer **11**; however, a significant degree of hydride shift was also observed leading to *cis*-1-chloro-4-methylcyclohexane (**15**) in nearly 1:1 ratio with the direct substitution product. We did not observe products resulting from a hydride-shift from the 2-positon (Table 3).

Importantly, in this 3-methylcyclohexanol system, we noted that the *cis*-isomer led to *cis*-only chlorination product. Not counting the hydride shift side reaction, we see that the *trans*-isomer gives only the *trans*-direct substitution product. These results do not seem to be consistent with a mechanism involving either neighboring group participation or diastereoselective attack on a carbocation as has been suggested for a related system.[12] If a classical S$_N$1 mechanism were operative

here, one would expect that both *trans*- and *cis*-alcohols would lead to the same product distribution which is not the case here.[13]
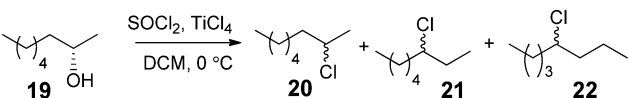
Our study of 4-methylcyclohexanols led to similar outcomes as the 3-methyl isomer system (Table 4). *Trans*-isomer **17** in this case was transformed in reasonable selectivity to *trans*-chlorinated product **16**. In an attempt to achieve exclusive retention of configuration, we performed extensive optimization resulting in a 7.5:1 product ratio in favor of stereo-retention. Under similar conditions, *cis*-isomer **18** gave *cis*-product **15** exclusively along with a nearly equal amount of hydride-shift isomer **13**. While our computational studies in the present work will only include a detailed analysis of the *trans*-4-methylcyclohexyl system, we note that the energy of the transition state involving *cis*-substrate **12** was the most stable (by 1.35 kcal/mol) of all the modeled transition states for 3- and 4-methylcyclohexyl isomers. This energetic preference may explain why only *cis*-3-methyl isomer **12** led to complete retention of configuration (Table 3).[14]

In our previous studies involving stereoretentive Ritter amidation reactions, we only observed stereoretentive results with cyclic secondary alcohols. As will be discussed below, we believe the current method is also mechanistically limited to cyclic secondary alcohol systems. Nevertheless, a limited study was performed on a nonracemic acyclic alcohol (Table 5). Starting with (*S*)-2-octanol (**19**), three chlorination products were observed resulting from direct substitution (**20**) as well as a hydride shift pathway (**21** and **22**). The hydride shift product could not be separated from the direct substitution product, and thus, its configuration could not be determined. However, our studies in a related system involving acyclic substrates suggest that the hydride shift product is likely racemic.[8] Assuming racemic hydride shift product, it appears that direct substitution chlorination product is formed as a near-racemic mixture as measured by optical rotation.

Table 4. Chlorination Results with *trans*-4-Methylcyclohexanol (17) and *cis*-4-Methylcyclohexanol (18)
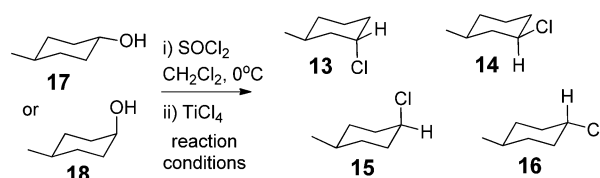
entry	ROH	conc (M)	temp (°C)	time (h)	TiCl$_4$ (equiv)	13:14:15:16[a]	yield[b] (%)
1	17	0.50	0	0.50	0.10	1.0:1.0:1.4:5.4	74
2	17	1.0	0	0.50	0.10	1.0:1.0:1.4:5.4	83
3	17	1.0	−78	2.0	2.0	1.0:1.0:1.4:5.4	73
4	17	0.050	0	1.0	1.0	2.0:1.0:2.5:13.7	72
5	17	0.10	0	0.50	0.20	2.0:1.0:2.5:13.7	80
6	17	0.10	0	0.50	2.0	5.0:1.0:8.5:49	76
7	17	0.10	−78	10	2.0	1.0:0:2.0:15	78
8	18	0.50	0	0.50	0.10	9.3:1.0:6.0:1.4	61
9	18	1.0	0	0.50	0.10	9.3:1.0:6.0:1.4	62
10	18	0.050	0	2.0	1.0	5.6:1.1:6.8:1.0	64
11	18	0.10	0	1.0	0.20	5.6:1.1:6.8:1.0	61
12	18	0.10	0	0.50	2.0	6.3:1.0:8.2:1.3	65
13	18	0.10	−78	2.0	2.0	64:1.5:62:1	60
14	18	1.0	−78	8.0	2.0	62:1.6:58:1.0	62

[a]Ratios determined by NMR. [b]Isolated yields. Relatively low yields likely due to product volatility since NMR analysis of crude indicates near quantitative conversion to the corresponding chloride.

**Table 5. Chlorination Results with (S)-2-Octanol[15]**

entry	conc (M)	time (h)	TiCl$_4$ (equiv)	$[\alpha]^a$	20:(21 + 22)	yield (%)
1	1.0	0.50	0.20	−2.6	1.2:1.0	90
2[b]	1.0	12	2.0	−3.5	1.0:1.0	77
3	0.10	1.0	1.0	+4.6	0.80:1.0	83
4	0.10	1.0	5.0	+4.4	0.80:1.0	83
5	0.10	1.0	10	+5.5	0.80:1.0	87
6	0.10	1.0	20	+5.7	0.80:1.0	93
7	0.050	24	0.20	−7.4	3.3:1.0	51
8	0.050	20	1.0	+4.3	0.90:1.0	60

^{a}Optical rotation of (R)-2-chlorooctane reported as −31.9 (4.5, CHCl$_3$). ^{b}Reaction temperature was −78 °C.

Traditional Chlorination Mechanisms. Perhaps the most salient feature of the present method is its limitation in stereoselectivity to cyclic alcohols only. To better understand this selectivity difference we first examine traditional ionic and concerted mechanisms in the chlorination of secondary alcohols with SOCl$_2$. Lewis and Boozer extensively studied chlorination reactions of alcohols with thionyl chloride.[16] They found that the configuration of the resulting chloride product was dependent on both reaction temperature and solvent and proposed a set of ionic mechanisms accounting for the different reaction conditions. When a chlorination reaction involving thionyl chloride and an alcohol is performed in a non-coordinating solvent (e.g., toluene) or neat, ionization of the chlorine−sulfur bond may occur (Scheme 2). However Lewis and Boozer argue that the loss of sulfur dioxide must be facilitated by the attack of chlorine ion from the back side of the carbinol carbon by an S$_N$2 mechanism.

Scheme 2. Lewis and Boozer Classic Mechanism for Alcohol Chlorination with SOCl$_2$
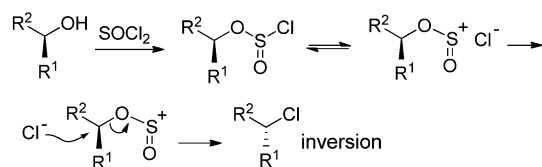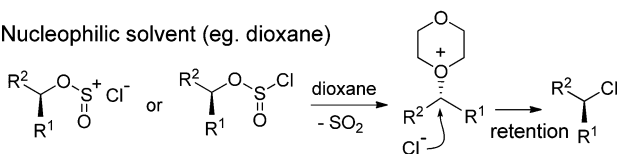
If a nucleophilic solvent such as dioxane is present, two consecutive S$_N$2 reactions take place leading to overall retention of configuration. Other non-nucleophilic solvents provide a solvating environment for the ionization of the chlorosulfite, and thus dissociation into ion-pairs is no longer prohibitively difficult. Depending on the polarity of the solvent involved, cleavage may take place at the chlorine−sulfur bond or the carbinol carbon−oxygen bond. Various pathways can then result including a front side, backside attack, or a combination of the two. As has often been observed, S$_N$1-type mechanisms are also possible leading to racemic chlorination of alcohols.[16b]

Pyridine has been reported as an exception to the typical behavior of nucleophilic solvents in the classical thionyl chloride reaction. Inversion of configuration is obtained from either the pyridinium chloride salt attacking from the backside of the chlorosulfite or the exchange between the pyridine and chloride of the chlorosulfite followed by the chlorine attacking from the backside.[17] We note that the reaction of l-menthol with thionyl chloride in refluxing dichloromethane led to the expected mixture of inversion and retention products in a ratio of 1:3.9 with an overall yield 82%. By contrast, the present methodology affords the menthyl chloride product with complete retention of configuration in 93% yield (Scheme 1).

Schleyer and co-workers reinvestigated the Lewis and Boozer hypotheses and offered a different mechanism based on frontier orbital theory. He argued that the nucleophilic chlorine atom was delivered from the chlorosulfite moiety via a 1,3-sigmatropic shift.[6c,18] In analyzing the possible shift geometries, he noted that a suprafacial 1,3-shift is both geometrically and symmetry allowed. Thus, a purely sigmatropic mechanism should lead to chlorination products with inversion of configuration without the intervention of nucleophilic solvents. However, this is often not the case, and thus many have concluded that the classical thionyl chloride reaction of alcohols proceeds by the originally proposed S$_N$i ionic mechanism.[19] Others have invoked similar mechanisms, the so-called S$_N$i backside or S$_N$2i.[20] However, in the present reaction involving the use of titanium tetrachloride, we have observed the opposite outcome than that predicted by the Lewis and Boozer mechanism; namely, predominantly retention products are obtained even though a noncoordinating solvent (dichloromethane) was used. There appears to be another factor in play with cyclic systems.

Hyperconjomer Theory. The work of Sorensen and co-workers on methylcyclohexyl tertiary carbocations suggests that these intermediates remain in a chair conformer (hyperconjomer) even after ionization.[21] In the present work, we note that whether the carbocation remains in the pyramidal configuration or distorts to a planar geometry may be a key factor in the stereochemical outcome of the reaction. Thus a carbocation might be generated under relatively mild conditions with the assistance of titanium tetrachloride. Invoking a Sorensen-type intermediate which does not transition to the planar geometry, we suggest that the cation continues to maintain the pyramidal orbital ready to capture the coming nucleophile from the less-hindered front face (Scheme 3).

The Sorensen group put forward two carbocation isomers with chair conformations, one isomer with a C−C bond distorted to maximize C$_\beta$−C$_\gamma$ hyperconjugation. The other conformer is stabilized through hyperconjugation by an adjacent C$_\beta$−H$_{ax}$ bond.[22] These two "hyperconjomers" can

Scheme 3. Hyperconjomer Intermediates Leading to Substitution Products
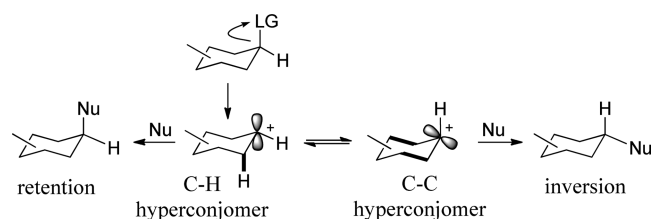
interconvert; thus, a key aspect influencing stereoselectivity in the present reaction would be the competition between the rate of the hyperconjomer interconversion and the rate of their nucleophilic capture.

We hypothesize that our titanium-promoted reactions involve chlorine from titanium capturing an empty orbital on the carbocation center. We further argue that the reaction proceeds via unique nonplanar carbocation mechanism in which the ionized substrate retains memory of its original configuration and is rapidly captured by a front side attack leading to the observed stereoretention outcome. At least for a brief instant, we suspect that the carbocation intermediate remains "frozen" in its original configuration under the mild conditions of its formation. As discussed in the next section, our computational data appear to confirm this line of reasoning. With sulfite-complexed TiCl$_4$ as the source of nucleophilic chlorine, an increase in the concentration of this Lewis acid should increase the rate of complex formation and subsequent cation capture at the expense of hyperconjomer interconversion (leading to an increase in stereoselectivity). This mechanistic interpretation is supported by our experimental studies especially involving the chlorination of 3,3,5-trimethylcyclohexanol (**7**) and β-cholestanol (**9**) (Table 2) where exclusive retentive product was obtained with added equivalents of titanium(IV) chloride.

For those substrates where the low energy conformation entails an hydroxyl group in an axial position, we observed a greater degree of hydride shift products. Presumably, hydride-shift (Wagner–Meerwein rearrangement) prefers hydride and leaving group to assume an anticoplanar arrangement.[23] Interestingly, both *cis*- and *trans*-3-methylcyclohexanols primarily led to the same *cis*-hydride shift chlorination product **15** (Table 3). Perhaps in this case the competition between nucleophilic capture and hydride-shift was somewhat equivalent. For reasons not well understood, the carbocation centers generated by the hydride shift appear to react with nucleophile to give to same chlorination product with both *trans*- and *cis*-3-methylcyclohexanol. A similar preference was observed for *trans*-H-shift product (**13**) over the *cis* (**14**) in chlorination reactions with *cis*- and *trans*-4-methylcyclohexanol (Table 4).

Computational Methods. Two different computational approaches were used in the present investigation: (i) the dimer method algorithm (DM)[24–27] as implemented in the CP2K package[28] and (ii) the "standard" Hessian–Newton–Raphson method[29] as implemented in the GAMESS software package.[30] The DM method has been already described in detail in the original work of Henkelman and Jónsson.[24] It is an energy surface-walking method able to evaluate the local curvature[24,26] of a potential energy surface using two symmetrically displaced atomic images of the system (the so-called "dimer"). Therefore, the lowest curvature of the potential energy surface, which corresponds to the lowest frequency normal mode,[31] is evaluated without the resource-intensive calculation and diagonalization of the Hessian (i.e., second derivatives of the potential energy). Due to its unique strategy, DM represents a useful approach to find transition states in a system involving a high number of degrees of freedom or a large periodic system (e.g., inorganic surfaces) where the numerical evaluation of the Hessian is computationally demanding.[25,27]

In this work, we manually built a set of guess structures, resembling a set of hypothetical transitions states guided by chemical intuition based on our previously related work

involving stereoretentive Ritter reactions.[8] Using DM, we then characterized an initial set of transition state structures. The obtained transition state conformations where then used as a starting point to characterize these states with the saddle-point-search module available with GAMESS. All calculations were performed by employing DFT level of theory, using PBE functional and the 6-31G** basis set (see the Experimental Section for additional computational details).

Computational Analysis of Carbocation Geometry. As described above, chlorination reactions of *cis*- and *trans*-3-methylcyclohexanol with SO$_2$Cl and TiCl$_4$ gave direct substitution products strongly favoring retention of configuration (Table 4). The *trans*-isomer seemed to be a simpler system which, under optimal conditions, gave only 6% of a single hydride shift byproduct. We thus chose this as a substrate to computationally examine two possible reaction paths leading to predominant retention of configuration (Figure 1a). In both
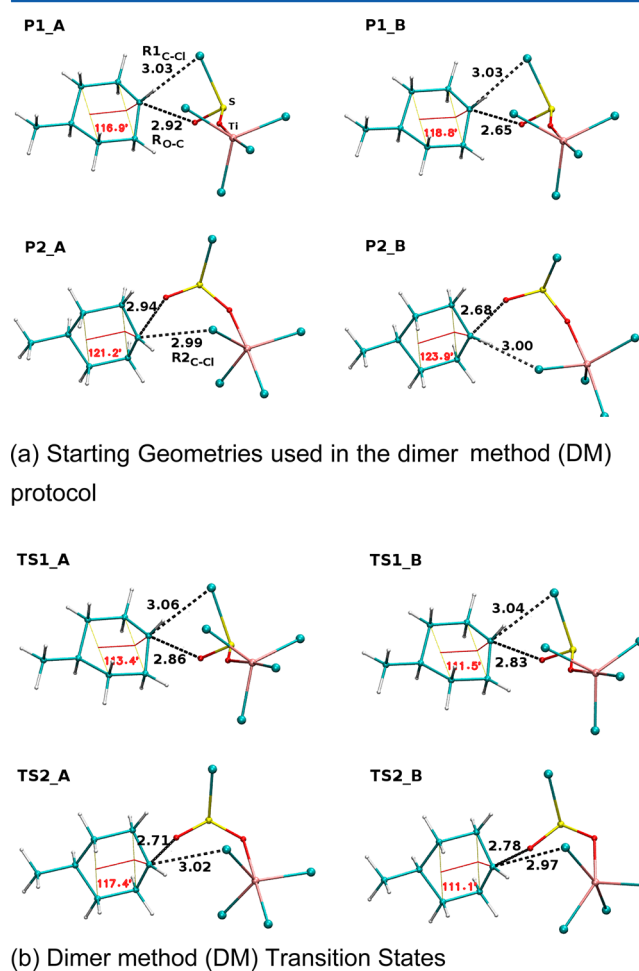

(a) Starting Geometries used in the dimer method (DM) protocol

(b) Dimer method (DM) Transition States

Figure 1. (a) Initial best-guess structures used for the dimer method (DM) calculation. (b) Transition-state geometries characterized using the DM. Angles (in red) are given in degrees and distances in Ångströms (Å).

hypotheses, the formation of the *trans*-3-methylcyclohexanoyl carbocation intermediate is followed by a nucleophilic attack by one chlorine atom. In one case, the attacking Cl originates from the chlorosulfite group and the reaction follows path 1 (system P1); in the other case, the Cl atom is provided by TiCl$_4$ and the reaction follows path 2 (system P2). Due to the high number of internal degrees of freedom of the system, two conformational

models (i.e., variant A and variant B) of each initial geometry were analyzed, while maintaining the alcohol ring unchanged in a chair conformation. Two transition states were characterized by using DM for both the P1 reaction path (i.e., DM-TS1_A and DM-TS1_B) and both the P2 reaction paths (i.e., DM-TS2_A and DM-TS2_B) (Figure 1b).

By comparing the transition states reported in Figure 1b, it was possible to recognize the main coordinates that define the reaction paths. For reaction path P1, these key coordinates are the distance between the "sulfinate oxygen" and the carbinol carbon atom of the *trans*-3-methylcyclohexanoyl moiety (R_{O-C}) and the distance between the carbinol carbon and the chlorine atom ($R1_{C-Cl}$) of the sulfinate group. For the reaction path P2, the key coordinate are the distance between the carbinol carbon and one of the chlorine atoms of $TiCl_4$ ($R2_{C-Cl}$) and the R_{O-C}.

The transition state conformational models (i.e., A and B) of each reaction path showed very small differences in the main coordinates and, in all cases, these conformations showed retention of configuration. The main coordinates defined above did not differ more than 0.07 Å, demonstrating that transition state variants of the same reaction path were essentially equivalent. In general, for all transition states, the R_{O-C} distance was found to be shorter than either the $R1_{C-Cl}$ or the $R2_{C-Cl}$ distances. These transition state geometries (Figure 1) are in reasonable agreement with the simplified front side attack models expounded in the work of Schreiner at the Hartree–Fock level of theory.[18b] We note, however, that the comparison of our results with those of Schreiner and co-workers is only approximate since the systems examined by those authors were significantly more simple (i.e., methyl chlorosulfite and ethyl chlorosulfite) than those of the present study. Perhaps more importantly, their system did not involve $TiCl_4$ and the calculations were performed at the Hartree–Fock level of theory.

One of the key hypotheses in the present work is that retention of configuration in the chlorination reaction is due to a nonplanar carbocation that is captured by the nucleophile while "frozen" in its original configuration. To computationally examine this mechanistic assertion, we monitored the geometrical values that define the conformation of the *trans*-3-methylcyclohexyl structure in order to understand how these putative nonplanar carbocations were stabilized.

The length of the C_β–C_γ and C_β–H_{ax} bonds and the carbocation out-of-plane angle (θ_1) are reported in Table 6 (see also Figures 2 and 3) for all transition states. In all cases, the C_β–C_γ bond lengths were stretched, the C_β–H_{ax} lengths were approximately at the equilibrium values of 1.10 Å and the angles θ_1 spanned a range of values between 110° and 120°. Our observed cyclohexyl geometry was consistent with a C_β-C_γ carbocation hyperconjomer as defined by Rauk and co-
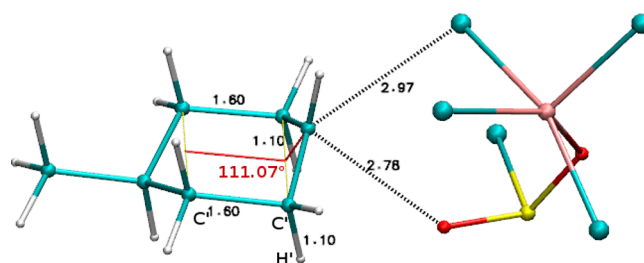

Figure 2. Ring geometry of nonplanar 4-methylcyclohexane carbocation. Angle θ_1 is shown in red.
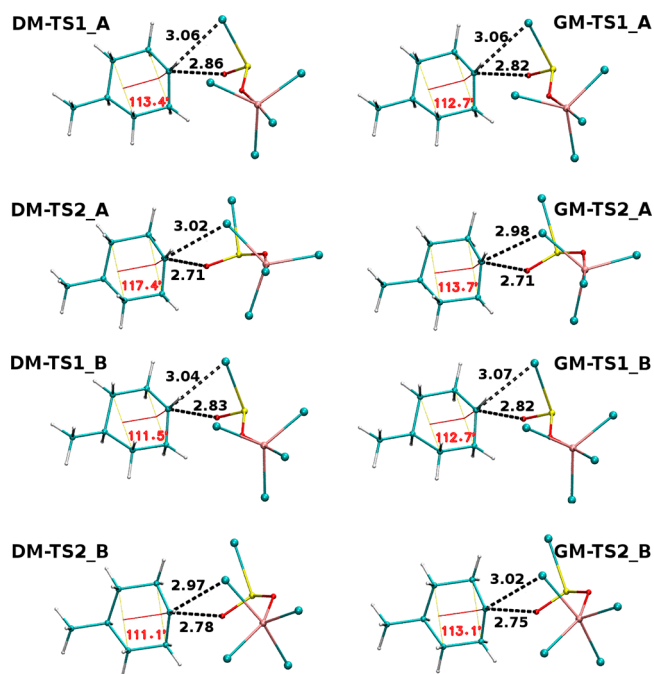

Figure 3. DM and GM transition states. Angles are given in degrees and distances in Å.

workers[22,32] and by Alabugin.[33] Combined with these previous reports, our findings suggests that these chlorination reactions proceed via the formation of a nonplanar carbocation species stabilized, in this case, as a C_β–C_γ hyperconjomer.

We next calculated energy levels with respect to structure DM-TS1_B, the transition state of lowest energy (Table 6). These energy differences did not exceed 4 kcal/mol; however, there appears to be a preference for reaction path P1 (by 2 kcal/mol). All the transition state structures obtained from DM calculations (DM-TS) were used as starting points to search for the saddle point using the SADPOINT module of the GAMESS updating the initial calculated Hessian matrix using the mixed Murtagh–Sargent–Powell method.[34] The obtained structures were characterized as transition state by calculating the proper number of imaginary harmonic vibrational frequencies.

The obtained DM transition states used as starting points and those verified by the GAMESS protocol (GM-TS) are shown in Figure 3 while the corresponding GM-TS geometrical values are reported in Table 7. The DM-TS structures were found to fit well with the GM transition state structures as demonstrated by the corresponding geometrical values (Figure 3) that showed only minor differences. The root-mean-square deviation (RMSD) of the GM transition states with respect to

Table 6. Transition-State Energies Relative to DM-TS1_B

transition states	C_β–C_γ (Å)	C_β–H_{ax} (Å)	θ_1 (deg)	relative energies (kcal/mol)
DM-TS2_A	1.593	1.100	113.4	3.9
	1.599	1.102		
DM-TS1_A	1.594	1.099	111.5	1.9
	1.600	1.101		
DM-TS2_B	1.592	1.099	117.4	2.2
	1.592	1.100		
DM-TS1_B	1.595	1.099	111.1	0
	1.597	1.100		

Table 7. Relative Energies with Respect to the GM-TS1_A/B

TS	RMSD (Å)	$C_\beta-C_\gamma$ (Å)	$C_\beta-H_{ax}$ (Å)	θ_1	relative energies (kcal/mol)	im freq (cm^{-1})
GM-TS2_A	0.2	1.594	1.099	113.7	2.5	168.96i
		1.595	1.099			
GM-TS1_A	0.17	1.593	1.099	112.7	0	176.63i
		1.599	1.101			
GM-TS2_B	0.08	1.596	1.099	113.1	2.3	170.37i
		1.595	1.100			
GM-TS1_B	0.07	1.594	1.099	112.7	0	147.87i
		1.599	1.100			

the initial starting conformations (i.e., DM transition states) were calculated as well (Table 7). These values are very small in magnitude especially for both the transition states of variant B.

Based on the geometrical values shown in Figure 3 and in Table 7, we argue that $C_\beta-C_\gamma$ bond lengths were maximized for all the characterized GM transition states. The $C_\beta-C_\gamma$ length values obtained for the GM transition states were very similar to those obtained for the DM transition states. Both transition state sets obtained from different protocol (i.e., GM-TS and DM-TS) were thus compatible with the $C_\beta-C_\gamma$ hyperconjomer confirming the "ionic nature" of the transition state in the present chlorination reaction.

We also calculated relative energy values with respect to the lowest transition state energy associated to the GM-TS1_A/B (Table 7). These values are in agreement with those described above (Table 6). The differences among the transition state energies did not exceed 3 kcal/mol and the preference for reaction path P1 was further confirmed.

The transition states of the pathways P1 and P2 were localized and validated by analysis of their imaginary vibrational frequencies. Furthermore, the TS conformations were used as starting point to relax the TS structures toward reactants and products by performing an intrinsic reaction coordinate (IRC) calculation with the IRC GAMESS module. This calculation is used to track the lowest energy path that connects the TS to the minimum conformation of the reactant and product species.[35]

The energy profiles of the reactions as obtained by IRC calculations were evaluated with respect to the local minimum reactant conformations of each reaction (Figure 5). As expected, the evaluated local energy minimums differed from each other. However, these differences did not exceed 0.4 kcal/mol; this difference is negligible compared to the relative activation energies of the observed energy profiles (Figure 4). Based on the activation energies calculated from these energy profiles, it appears that reaction P1 is favored over reaction P2 by 3 kcal/mol (Figure 4).

The energy profile for a chlorination reaction was also modeled without TiCl$_4$ (black curve, Figure 4). The transition state conformation for this metal-free reaction was also modeled (Figure 5) and, as expected, the reaction path without TiCl$_4$ (P0) proceeded in a manner similar to reaction path P1. Transition state P0 (TS0), however, was found to be destabilized by 9 kcal/mol with respect to the TS1, and 6 kcal/mol with respect to TS2. We conclude this observed destabilization is due to the absence of TiCl$_4$. This computational result is not surprising given the observed catalytic effect of TiCl$_4$ in the present reaction.

According to the just described computational results, the P1 reaction proceeded from reactants to give chlorinated
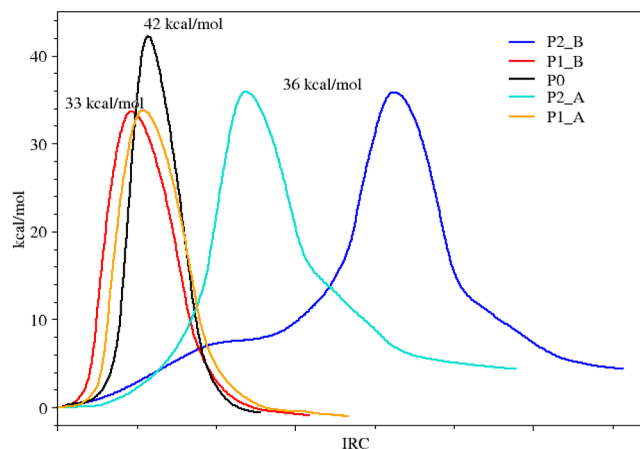

Figure 4. Reaction energy profiles including one reaction without TiCl$_4$ (transition state for the reaction with profile P0 is depicted in Figure 5). All energies profiles are evaluated with respect to the reactant energies.
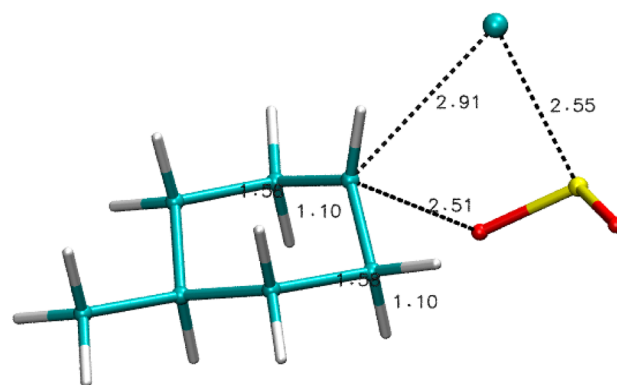

Figure 5. Transition state for the chlorination reaction without TiCl$_4$ (GM-TS0) was characterized with the saddle point search of GAMESS. Distances are in Å.

compound and the OSO−TiCl$_4$ complex. These products were more stable than the reactants by 1 kcal/mol for both reaction variants P1_A and P1_B. The TiCl$_4$ did not take part directly in the chlorination reaction, therefore it was in a relaxed conformation and the titanium atom was in a "*trans*" conformation with respect to the nucleophilic alcohol oxygen of the sulfinate fragment. The *trans*-conformation minimized the steric effects between TiCl$_4$ and cyclic alcohol segment (see Figures 1 and 2). In the P1 reaction, therefore, the TiCl$_4$ promoted only the formation of the TS by stabilizing the negative charge in the sulfinate fragment.

The P2 reaction proceeded from the reactants toward the chlorinated compound and the Cl$_3$Ti/OSOCl intermediate compound. The reaction was completed by an additional reaction step in which chlorine atom left the SO$_2$Cl intermediate to restore the TiCl$_4$ catalyst. For variant reactions A and B, the energy difference between the intermediate products and the reactants was 3 kcal/mol in favor of reactants. In the P2 reaction, TiCl$_4$ was directly involved in the reaction and titanium atom was in the "*cis*" conformation with respect to the oxygen atom. The cis-conformation seemed to "chelate" the carbocation minimizing the distance between carbocation and the Cl atoms of the TiCl$_4$ favoring nucleophilic attack. The P2 mechanism used the TiCl$_4$ fragment to perform the nucleophilic attack; therefore, it involved more degrees of

freedom than the P1 mechanism. As a consequence, the P2 energy profiles showed a longer and more complex IRC than the P1 energy profiles (see Figure 4). In particular, the P2_B profile highlighted a sort of "hump" during the relaxation toward reactants. Observing the IRC trajectory we realized that this energy "hump" was due to a partial rotation of the TiCl$_4$ along the Ti−O bond. By exploiting this degree of freedom the system was able to place one of the Cl atom of the TiCl$_4$ toward the carbocation, promoting the nucleophilic attack. The presence of TiCl$_4$ in the vicinity of the "frozen carbocation" increased the probability of finding an atom of chlorine to perform the nucleophilic attack, favoring the P2 reaction from a statistical point of view

The interaction energy between the carbocation in the present investigation (i.e., *trans*-4-methylcyclohexyl moiety) and the fragment comprised of SO$_2$Cl and TiCl$_4$ were studied using the localized molecular orbital-energy decomposition analysis (LMO-EDA) implemented by Su and Li in the GAMESS software[36] for transition state structures of type A (i.e., GM-TS2_A GM-TS1_A) and the structure of the reaction modeled without TiCl$_4$ (i.e., GM-TS0). We computed the decomposition of the total interaction energy ΔE_{tot} between two fragments of each transition state into electrostatic (ΔE_{elec}), exchange (ΔE_{ex}), repulsion (ΔE_{rep}), polarization (ΔE_{pol}), and dispersion (ΔE_{disp}) components (Table 8).

Table 8. Decomposition of Interaction Energies (kcal/mol) for Type A Transition States and for Transition State GM-TS0 for the Reaction Modeled without TiCl$_4$

TS	ΔE_{tot}	ΔE_{elec}	ΔE_{ex}	ΔE_{rep}	ΔE_{pol}	ΔE_{disp}
GM-TS2_A	−79.67	−73.89	−4.68	27.16	−22.29	−5.96
GM-TS1_A	−82.6	−75.8	−4.14	25.24	−21.17	−6.7
GM-TS0	−105.69	−93.97	−6.4	36.5	−35.27	−6.55

Interaction energies were inversely proportional to the relative ΔG^* calculated in the present reaction (Figure 4). The best interaction energy was observed with GM-TS0. In all cases, the total interaction energies were dominated by the electrostatic component (ΔE_{elec}), suggesting that the interaction energies between the two fragments is mainly electrostatic. The relatively small values of ΔE_{pol} suggest that interactions between fragments are not covalent in nature.[36] Moreover, using this computational technique, one can argue that the differences between the GM-TS0 (without TiCl$_4$) and the other transition states modeled with TiCl$_4$ rely mainly in the ΔE_{elec} component. This finding demonstrates that TiCl$_4$ favors carbocation formation by stabilizing the negative charge on SO$_2$Cl and consequently decreases the activation energy of the reaction.

Finally, we sought to evaluate the possibility raised by Schleyer and co-workers that reactions of chlorosulfites follow a concerted mechanism.[6c] To this end, the highest occupied molecular orbitals (HOMOs) and lowest unoccupied molecular orbitals (LUMOs) of transition state structures GM-TS1_A and GM-TS2_A were generated (Figure 6). The depicted HOMOs (and that of other related transition states) showed that the occupied molecular orbital were mainly localized in the chlorine atoms capable of attacking the trans-3-methylcyclohexanol carbocation and in the nucleophilic oxygen atom linked to the cyclohexyl skeleton. The LUMOs for transition state
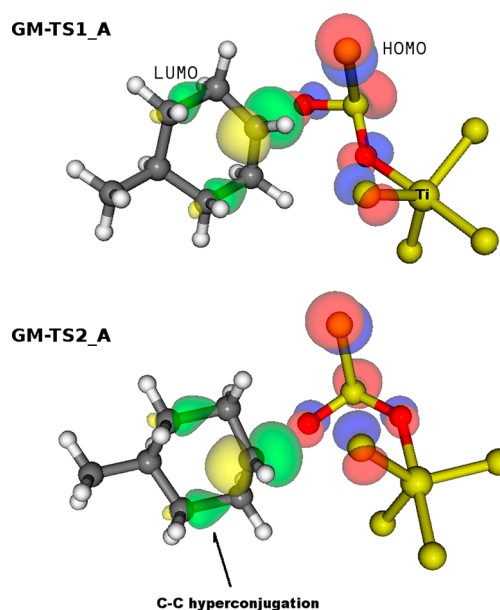

Figure 6. HOMO/LUMO orbitals for GM-TS1_A and GM-TS2_A. HOMO orbitals are depicted in red/blue, whereas LUMO are depicted in green/yellow.

structures GM-TS1-A and GM-TS2_A (and that of other related transition states) showed the characteristic C_β−C_γ hyperconjugation orbitals[32] with the large p-orbitals localized on the carbon atoms undergoing nucleophilic attack. As expected, the molecular orbitals and those in all transition states described in this work show no significant orbital overlap between the HOMO and LUMO orbitals. This suggests the present chlorination reaction is not likely to proceed by a concerted (orbital controlled) pathway as suggested by the previous LMO-EDA analysis.

Based on our computational results and experimental findings, we put forward the following mechanism for the TiCl$_4$ catalyzed chlorination *trans*-4-methylcyclohexanol and by extension other cycloalkanols reported in this study. An alkyl chlorosulfite generated in situ initially undergoes complexation with the Lewis acid at the sulfoxyl oxygen (Scheme 4). This

Scheme 4. Proposed Mechanism for the Stereoretentive Chlorination of Cyclohexanols
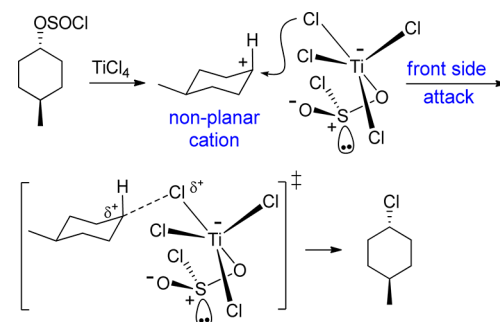
complex proceeds to form a nonplanar carbocation intermediate that is stabilized though hyperconjugation. This stabilization allows the carbocation to maintain its configuration under the reaction conditions long enough to be captured by a chloride ion delivered to the front side by the titanium(IV)−OSOCl leaving group (Scheme 4). Computational evidence

suggests that carbocation generation and its subsequent capture by chloride do not occur as part of a concerted mechanism.

■ CONCLUSIONS

We have discovered an exciting modification of the well-known and widely used alcohol chlorination reaction using thionyl chloride. An important element of design in this new reaction was the idea that chlorosulfites formed in situ could serve as leaving groups capable of chelating the $TiCl_4$ catalyst. The new protocol leads to chlorination products in high yields under milder conditions than the classical thionyl chloride reaction. In most cases, these optimal results were obtained with catalytic amounts of the Lewis acid. With chiral cyclic alcohols, the reaction primarily yields products with retention of configuration raising mechanistic questions which we sought to examine using computational methods. In this regard, two different stereoretentive reaction mechanisms were investigated using the dimer method as implemented in CP2K and the SADPOINT module of the GAMESS. The transition-state structures resulting from these approaches showed unambiguously that both reaction pathways (i.e., P1 and P2) took place through the formation of the C_β-C_γ hyperconjomer. The agreement between the results indirectly validated the DM algorithm implemented in CP2K and showed that DM can be efficiently used to characterize very difficult transition states. The presence of $TiCl_4$ in both cases stabilized the formation of the carbocation providing evidence for the catalytic role of the Lewis acid. Both pathways were compatible with a mechanism in which the carbocation appears "frozen" in a nonplanar geometry. The P2 reaction involved more degrees of freedom than P1 reaction, with the $TiCl_4$ providing a nucleophilic chlorine atom in more ways than the SO_2Cl alone. Because a higher number of equivalent reaction paths of the kind P2 can occur, an entropic contribution under experimental condition likely offsets the observed difference in destabilization potential energy relative to the P1 mechanism. Though proceeding through a less favored transition state (3 kcal/mol) than that of P1, we argue that the P2 pathway is favored in the "real reaction environment". Ultimately, this work puts forward a modified conception of carbocation chemistry and a first practical application of hyperconjomer theory. Further studies on this system are currently underway especially with a view to improving stereoselectivity and expanding substrate generality.

■ EXPERIMENTAL SECTION

General Procedure for Chlorination (High Concentration). To an argon-blanketed and ice-cooled solution of alcohol (1.0 equiv) in dichloromethane (1.0 M) was added thionyl chloride (1.5 equiv). Hydrogen chloride, which is generated during this step, was vented from the reaction. After 1 h, $TiCl_4$ was added (catalytic to stoichiometric amounts) and stirred for the required time (usually 15 min). The reaction mixture was quenched with water, stirred until both layers were clear, and extracted three times with dichloromethane. The collected organic extracts were concentrated, and the resulting oil was purified by silica gel chromatography (usually using pure hexanes as eluent).

General Procedure for Diluted Chlorination Reactions. To an ice-cold 1.0 M solution of alcohol in dichloromethane was added thionyl chloride (1.5 equiv) and stirred for 1 h. Hydrogen chloride which is generated during this step was vented from the reaction. The reaction mixture was then diluted to the required concentration (usually 0.5 or 0.01 M) by adding the required amount dichloromethane via syringe and cooled to the required temperature (usually −78 or 0 °C). After 1 h, $TiCl_4$ was added (catalytic to stoichiometric

amounts) and stirred for the required time. The reaction mixture was quenched with water, stirred until both layers were clear, and extracted three times with dichloromethane. The collected organic extracts were concentrated and the resulting oil was purified by silica gel chromatography (usually using pure hexanes as eluent).

(1R, 2R)-1-Chloro-2-methylcyclohexane (racemic): ^{1}H NMR (400 MHz, CDCl$_3$) δ 3.53−3.47 (td, J = 10.59, 4.19 Hz, 1H), 2.25−2.17 (m, 1H), 1.83−1.74−1.71 (m, 2H), 1.68−1.54 (m, 4H),1.31−1.24 (m, 2H), 1.07(d, J = 6.47 Hz, 3H); ^{13}C NMR (100 MHz, CDCl$_3$) δ 67.7, 41.1, 37.5, 34.8, 26.5, 25.4, 20.2. Known compound.[37]

(1S, 3R)-1-chloro-3-methylcyclohexane (racemic): ^{1}H NMR (400 MHz, CDCl$_3$) δ 3.88−3.80 (tt, J = 11.69, 4.14 Hz, 1H), 2.19−2.14 (m, 2H), 1.82−1.75 (m, 1H), 1.66−1.61 (m, 1H),1.53−1.41 (m, 2H), 1.33−1.21 (m, 2H), 0.92 (d, J = 6.54 Hz, 3H), 0.90−0.80 (m, 1H); ^{13}C NMR (100 MHz, CDCl$_3$) δ 59.7, 45.9, 36.9, 33.5, 33.1, 25.9, 22.2. Known compound.[38]

(1R, 3R)-1-chloro-3-methylcyclohexane (racemic): ^{1}H NMR (400 MHz, CDCl$_3$) δ 4.50−4.47 (b m, 1H), 1.99−1.89 (m, 3H), 1.82−1.65 (m, 3H), 1.57−1.52 (m, 1H),1.45−1.38 (m, 1H),0.99−0.93 (m, 1H), 0.89 (d, J = 6.53 Hz, 3H); ^{13}C NMR (100 MHz, CDCl$_3$) δ 60.1, 42.3, 34.1, 33.9, 26.4, 21.7, 20.2. Known compound.[39]

trans-1-Chloro-4-methylcyclohexane (racemic): ^{1}H NMR (400 MHz, CDCl$_3$) δ 3.85−3.77 (tt, J = 11.60, 4.19 Hz, 1H), 2.19−2.14 (m, 2H), 1.77−1.73 (m, 2H), 1.67−1.59 (m, 2H),1.44−1.35 (m, 1H), 1.06−0.96 (m, 2H), 0.87(d, J = 6.56 Hz, 3H); ^{13}C NMR (100 MHz, CDCl$_3$) δ 60.1, 37.1, 34.8, 31.2, 21.8. Known compound.[39]

cis-1-Chloro-4-methylcyclohexane (racemic): ^{1}H NMR (400 MHz, CDCl$_3$) δ 4.42−4.39 (b m, 1H), 1.98−1.93 (m, 2H), 1.81−1.73 (m, 2H), 1.51−1.43(m, 5H), 0.93(d, J = 5.29 Hz, 3H); ^{13}C NMR (100 MHz, CDCl$_3$) δ 59.8 33.6, 28.9, 22.3, 14.0. Known compound.[39]

(1S, 5S)-1-chloro-3,3,5-trimethylcyclohexane (racemic): ^{1}H NMR (400 MHz, CDCl$_3$) δ 4.07−3.99 (tt, J = 12.11, 4.19 Hz, 1H), 2.19−2.13 (m, 1H), 1.91−1.86 (m, 1H), 1.70−1.61 (m, 1H), 1.36−1.31 (m, 2H), 1.18−1.09 (m, 1H), 0.95 (s, 3H), 0.91 (d, J = 6.51 Hz, 3H), 0.90 (s, 3H), 0.84−0.78 (m, 1H); ^{13}C NMR (100 MHz, CDCl$_3$) δ 57.4, 49.5, 46.9, 45.7, 33.4, 32.8, 28.7, 25.1, 22.1.

Computational Details. Calculations were performed with the CP2K/Quickstep[40−42] and with GAMESS[30] software packages. The results were visualized with Molekel[43] or VMD[44] software packages. All calculations were performed at the DFT level of theory using the PBE functional[45] and the 6-31G** basis set. CP2K calculations were performed within the Gaussian-augmented-plane-wave (GAPW)[42] framework and by using a density cutoff 280 Ry. Energies were tested for convergence with respect to the wave function gradient of 10^{-6} hartree. All CP2K calculations were performed in vacuum without periodic boundary conditions using Martyna−Tuckerman (MT) Poisson solver.[46] Molecular complexes were placed into the box center. During calculations the molecular system dimension remain within a box 11 × 6 × 6 Å. Accordingly with the Martyna−Tuckerman specifications,[46] a box of 24 × 15 × 15 Å was used to achieve a zero electronic density at the edge of the box.

To determine the transition states were used the dimer method[24] implemented in CP2K and the SADPOINT module of the GAMESS packages. The DM calculation in CP2K was activated specifying DIMER as method in TRANSITION_STATE subsection of geometrical optimization (GEO_OPT) section. The conjugate gradient (CG) algorithm was used to minimize the angle rotation and to translate the dimer. Based on our experience the dimer separation value DR was set to 0.005 Å and the tolerance for rotational angle convergence was set to 1.0 degrees. During optimization of the dimer rotation the gradient was interpolated activating the INTERPOLATE_GRADIENT Boolean keyword. Root mean square (RMS) values of 0.0003 hartree/Bohr for force and 0.0003 Bohr for positions were selected as convergence criteria.

The transition states calculated with GAMESS were fully optimized with gradient convergence set to 0.0003 Hartree/Bohr. In the saddle point searches, the Hessian was updated with the mixed Murtagh−Sargent/Powell procedure.[34] Imaginary frequencies and intrinsic reaction coordinate calculations were used to verify the adjacent local minima. The IRC were traced at the same level of theory and

tolerance criteria from transition states toward both reactants and products directions using the Gonzalez−Schlegel algorithm.[35]

■ ASSOCIATED CONTENT

Ⓢ Supporting Information

Copies of NMR spectra for entries in Tables 1 − 5 including calculations of molar ratios of chlorinated isomers. Computational details and coordinates for the TSs obtained from the DM and GM procedures. Movie showing the IRC trajectories for reactions P2_B and P1_B (reported in Figure 5). This material is available free of charge via the Internet at http://pubs.acs.org.

■ AUTHOR INFORMATION

Corresponding Author

*E-mail: slepore@fau.edu, luca.bellucci_s3@unimore.it.

Notes

The authors declare no competing financial interest.

■ ACKNOWLEDGMENTS

■ REFERENCES

(1) (a) Yasuda, M.; Onishi, Y.; Ueba, M.; Miyai, T.; Baba, A. *J. Org. Chem.* **2001**, *66*, 7741. (b) Yasuda, M.; Saito, T.; Ueba, M.; Baba, A. *Angew. Chem., Int. Ed.* **2004**, *43*, 1414.

(2) (a) *Comprehensive Organic Transformations*, 1st ed.; Larock, R. C., Ed.;Wiley-VCH: New York, 1989; p 353. (b) Lewis, E. S.; Boozer, C. E. *J. Am. Chem. Soc.* **1952**, *74*, 308. (c) Hepburn, D. R.; Hudson, H. R. *J. Chem. Soc., Perkin Trans. 1* **1976**, 754. (d) Gomez, L.; Gellibert, F.; Wagner, A.; Mioskowski, C. *Tetrahedron Lett.* **2000**, *41*, 6049.

(3) For a review of $SOCl_2$, see: Pizey, J. S. *Synth. Reagents* **1974**, *1*, 321.

(4) (a) Denton, R. M.; An, J.; Adeniran, B. *Chem. Commun.* **2010**, *46*, 3025. (b) Sekar, G.; Nishiyama, H. *J. Am. Chem. Soc.* **2001**, *123*, 3603. (c) Kozikowski, A. P.; Lee, J. *Tetrahedron Lett.* **1988**, *29*, 3053.

(5) (a) Lewis, E. S.; Boozer, C. E. *J. Am. Chem. Soc.* **1952**, *74*, 308. (b) Boozer, C. E.; Lewis, E. S. *J. Am. Chem. Soc.* **1953**, *75*, 3182. (c) Lewis, E. S.; Coppinger, G. M. *J. Am. Chem. Soc.* **1954**, *76*, 796.

(6) (a) Cram, D. J. *J. Am. Chem. Soc.* **1953**, *75*, 332. (b) Cowdrey, W. A.; Hughes, E. D.; Ingold, C. K.; Masterman, S.; Scott, A. D. *J. Chem. Soc.* **1937**, 1252. (c) Schreiner, P.; Schleyer, P. R.; Hill, R. K. *J. Org. Chem.* **1993**, *58*, 2822.

(7) (a) Lepore, S. D.; Bhunia, A. K.; Mondal, D.; Cohn, P. C.; Lefkowitz, C. *J. Org. Chem.* **2006**, *71*, 3285. (b) Lepore, S. D.; Mondal, D.; Li, S. Y.; Bhunia, A. K. *Angew. Chem., Int. Ed.* **2008**, *47*, 7511.

(8) Mondal, D.; Bellucci, L.; Lepore, S. D. *Eur. J. Org. Chem.* **2011**, 7057.

(9) Unpublished results.

(10) We also examined chlorination reactions with (+)-neomenthol and *cis*-2-methylcyclohexanol where hydroxyl groups are in the axial position in the preferred conformation. In those cases, addition of thionyl chloride at 0 °C led to a mixture of elimination and tertiary chloride products very rapidly. Attempts to form chlorosulfites at −78 °C were unsuccessful.

(11) When treated under typical thionyl chloride conditions (benzene, rt), this substrate was converted to tertiary chloride as the major product.

(12) Braddock, D. C.; Pouwer, R. H.; Burton, J. W.; Broadwith, P. *J. Org. Chem.* **2009**, *74*, 6042.

(13) (a) Cozzi, P. G.; Benfatti, F. *Angew. Chem., Int. Ed.* **2010**, *49*, 256. (b) Muhlthau, F.; Stadler, D.; Goeppert, A.; Olah, G. A.; Prakash, G. K. S.; Bach, T. *J. Am. Chem. Soc.* **2006**, *128*, 9668.

(14) Assuming pathway 2 (see the Computational Methods), the relative energies (kcal/mol) of the transition states for these four cyclohexyl isomers are as follows: *cis*-3-methyl (0), *trans*-4-methyl (1.35), *cis*-4-methyl (2.02), and *trans*-3-methyl (2.13). See the Supporting Information.

(15) Munyemana, F.; Frisque-Hesbain, A.; Devos, A.; Ghosez, L. *Tetrahedron Lett.* **1989**, *30*, 3077.

(16) (a) Lewis, E. S.; Boozer, C. E. *J. Am. Chem. Soc.* **1952**, *74*, 308. (b) Boozer, C. E.; Lewis, E. S. *J. Am. Chem. Soc.* **1953**, *75*, 3182.

(17) Walden, P. R. Z. *Anorg. Chem.* **1900**, *25*, 209.

(18) Schreiner, P. R.; Schleyer, P. R.; Hill, R. K. *J. Org. Chem.* **1994**, *59*, 1849.

(19) (a) Wallis, E. S.; Bowman, P. I. *J. Org. Chem.* **1936**, *1*, 383. (b) Roberts, J. D.; Young, W. G.; Winstein, S. *J. Am. Chem. Soc.* **1942**, *64*, 2157. (c) Winstein, S.; Morse, B. K.; Grunwald, E.; Schreiber, K. C.; Corse, J. *J. Am. Chem. Soc.* **1952**, *74*, 1113.

(20) Moss, R. A.; Fu, X.; Tian, J.; Sauers, R.; Wipf, P. *Org. Lett.* **2005**, *7*, 1371.

(21) Kirchen, R. P.; Ranganayakulu, K.; Sorensen, T. S. *J. Am. Chem. Soc.* **1987**, *109*, 7811.

(22) Rauk, A. R.; Sorensen, T. S.; Schleyer, P. R. *J. Chem. Soc., Perkin Trans. 2* **2001**, *6*, 869.

(23) Sun, X. *Symmetry* **2010**, *2*, 201.

(24) Henkelman, G.; Jónsson, H. *J. Chem. Phys.* **1999**, *111*, 7010.

(25) Heyden, A.; Bell, A. T.; Keil, F. J. *J. Chem. Phys.* **2005**, *123*, 224101.

(26) Henkelman, G.; Johannesson, G.; Jónsson, H. *J. Theor. Methods Condensed Phase Chem.* **2002**, 269.

(27) Kastner, J.; Sherwood, P. *J. Chem. Phys.* **2008**, *128*, 14106.

(28) The CP2K developers group, http://cp2k.berlios.de (accessed June 2, 2009).

(29) Jensen, F. *Introduction to Computational Chemistry*; Wiley: New York, 2007.

(30) Schmidt, M. W.; Baldridge, K. K.; Boatz, J. A.; Elbert, S. T.; Gordon, M. S.; Jensen, J. H.; Koseki, S.; Matsunaga, N.; Nguyen, K. A.; Su, S.; et al. *J. Comput. Chem.* **1993**, *14*, 1347.

(31) Voter, A. F. *Phys. Rev. Lett.* **1997**, *78*, 3908.

(32) Rauk, A.; Sorensen, T. S.; Maerker, C.; de M. Carneiro, J. W.; Sieber, S.; Schleyer, P. v. R. *J. Am. Chem. Soc.* **1996**, *118*, 3761.

(33) Alabugin, I. V.; Manoharan, M. *J. Org. Chem.* **2004**, *69*, 9011.

(34) Murtagh, B. A.; Sargent, R. W. H. *Comput. J.* **1970**, *13*, 185.

(35) Gonzalez, C.; Schlegel, H. B *J. Phys. Chem.* **1990**, *94*, 5523.

(36) Su, P.; Li, H. *J. Chem. Phys.* **2009**, *131*, 014102.

(37) Monnier, M.; Aycard, J. P. *Can. J. Chem.* **1979**, *57*, 1257.

(38) Heumann, A.; Baeckvall, J. E. *Angew. Chem.* **1985**, *97*, 228.

(39) Schneider, H. J.; Hoppen, V. *J. Org. Chem.* **1978**, *43*, 3866.

(40) Lippert, G.; Hutter, J.; Parrinello, M. *Theor. Chem. Acc.* **1999**, *103*, 124.

(41) See ref 28.

(42) VandeVondele, J.; Krack, M.; Mohamed, F.; Parrinello, M.; Chassaing, T.; Hutter, J. *Comput. Phys. Commun.* **2005**, *167*, 103.

(43) Varetto, U. Molekel 5.4.0.8; Swiss National Supercomputing Centre: Manno (Switzerland).

(44) Humphrey, W.; Dalke, A.; Schulten, K. *J. Mol. Graph.* **1996**, *14*, 33.

(45) Perdew, J. P.; Burke, K.; Ernzerhof, M. *Phys. Rev. Lett.* **1996**, *77*, 3865.

(46) Martyna, G. J.; Tuckerman, M. E. *J. Chem. Phy.* **1999**, *110*, 2810.